Research article

JHEP|Reports

Progressive fibrosis in human MASLD is associated with spatially linked transcriptomic signatures of metabolic reprogramming and senescence

Authors

Hani Vu, Yuliangzi Sun, Zherui Xiong, …, Katharine M. Irvine, Quan H. Nguyen, Elizabeth E. Powell

Correspondence

Elizabeth.Powell@qimrb.edu.au (E.E. Powell), Quan.Nguyen@qimrb.edu.au (Q.H. Nguyen), katharine.irvine@uq.edu.au (K.M. Irvine).

Graphical abstract

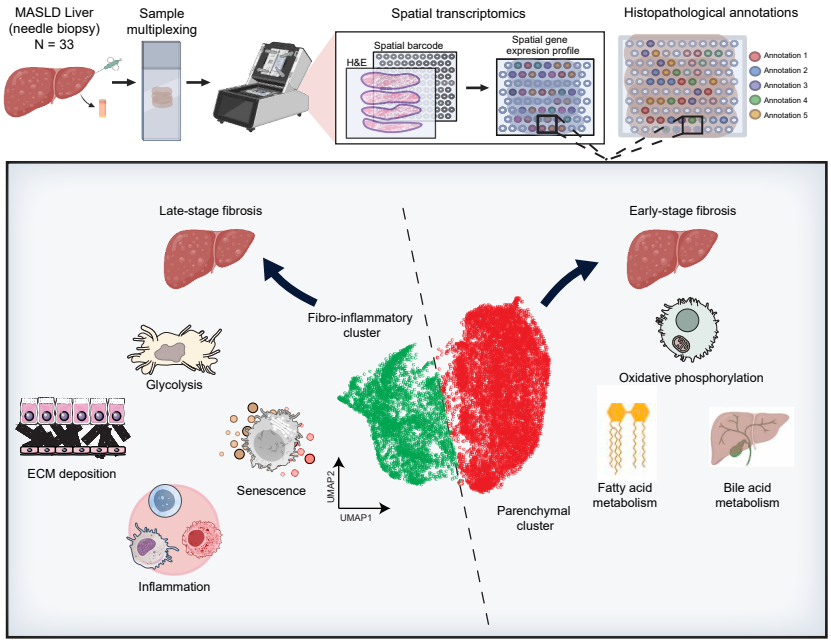

Highlights:

- Spatial transcriptomics identified expression signatures of histopathological features of MASLD progression.
- Fibroinflammatory regions were spatially associated with a senescence signature.
- Senescent regions exhibited increased immunoglobulin gene expression and evidence of metabolic perturbations.

Impact and implications:

Metabolic dysfunction-associated steatotic liver disease (MASLD) has a complex pathogenesis driven by cell and matrix interactions in inflammatory niches. In this study, we identify a senescence signature in fibroinflammatory regions, characterised by high immunoglobulin expression and associated with a shift from oxidative to glycolytic metabolism. We identify spatially co-expressed ligand-receptor pairs, including senescence-associated factors, correlated with progressive fibrosis. This discovery dataset highlights the complex cross-talk between metabolic perturbations and inflammation underpinning fibrosis progression in MASLD and lays the groundwork for future research into the role of senescence in MASLD.

https://doi.org/10.1016/j.jhepr.2025.101657

Research article

JHEP|Reports

Progressive fibrosis in human MASLD is associated with spatially linked transcriptomic signatures of metabolic reprogramming and senescence

Hani Vu[1,2], Yuliangzi Sun[2], Zherui Xiong[1,2], Xiao Tan[1,2], Daniel Radford-Smith[3], Andrew Causer[1,2], Alex M. Dickens[4,5], Tuulia Hyötyläinen[6], Ilia Evstafev[4], Matej Oresic[4,7,8], Christian Nefzger[2], Eoin D. O'Sullivan[1,9], Matthew J. Watt[10], Grant A. Ramm[1], Andrew Clouston[11], Katharine M. Irvine[12,*], Quan H. Nguyen[1,2,*], Elizabeth E. Powell[1,11,13,*]

JHEP Reports **2026**. vol. 8 | 1–12

Background & Aims: Granular detail about the location and nature of liver cell interactions and the metabolic, inflammatory and fibrogenic pathways driving progressive fibrosis in metabolic dysfunction-associated steatotic liver disease (MASLD) is needed to identify novel therapeutic targets.

Methods: We generated Visium spatial transcriptomic data from 33 human liver biopsies across the spectrum of MASLD. Gene expression data were overlaid with histological annotations to integrate spatial molecular and histopathological information, enabling interrogation of disease progression. Differential gene expression, pathway, cellular deconvolution and ligand-receptor interaction analyses were conducted for each annotated anatomical category, with specific protein expression validated using immunohistochemistry staining.

Results: Unsupervised clustering based on gene expression data classified the annotated spots into two main clusters enriched for fibro-inflammatory *vs*. parenchymal regions. Transcriptomic cellular deconvolution aligned well with manually annotated histopathological features. Fibrotic regions were enriched for genes involved in extracellular matrix/receptor interactions and inflammatory pathways (Benjamini-Hochberg adjusted p values <0.05), underscoring known pathological mechanisms. We also identified immunoglobulin gene induction in late-stage fibrosis, which was spatially associated with a senescence signature, as has previously been reported in aging tissues. Dynamic changes in metabolic gene expression from early to late fibrosis were observed, suggesting MASLD progression is accompanied by a decline in normal liver metabolic function and reprogramming of metabolic fuel utilisation from oxidative to glycolytic metabolism, which may be both a cause and a consequence of senescence.

Conclusions: Taken together, our valuable discovery dataset highlights the complex crosstalk between metabolic perturbations and inflammation underpinning fibrosis progression in MASLD.

Introduction

Metabolic dysfunction-associated steatotic liver disease (MASLD) is the leading cause of chronic liver disease, and a risk factor for cardiovascular events and kidney disease.[1] MASLD covers a spectrum of phenotypes, ranging from fatty (steatotic) liver without significant inflammation, to metabolic dysfunction-associated steatohepatitis (MASH) in which hepatic steatosis is associated with liver cell injury and inflammation, with or without fibrosis.[2] Patients with progressive liver fibrosis are at risk of developing cirrhosis, which in turn can lead to liver failure and hepatocellular carcinoma (HCC), a form of cancer whose global incidence is rapidly increasing.[1]

MASLD has a complex pathophysiology: in a background of rising hepatic fat and increasing insulin resistance, inflammatory signals circulate between the liver, adipose tissue and gastrointestinal tract.[3] These signals paradoxically increase hepatic fat production and storage, ultimately resulting in the generation of toxic lipids that drive hepatocyte damage, inflammation and fibrogenesis. As MASLD progresses, increasing fibrosis disrupts the architecture of the liver, leading to cirrhosis and the associated risk of liver failure and HCC. Key cellular mechanisms of MASLD progression include hepatocyte cell death, activation of liver-resident macrophages, immune cell infiltration, and activation of hepatic stellate cells that promote fibrogenesis.[4]

In March 2024, the FDA approved the first drug (resmetirom) for the treatment of MASH with moderate to advanced fibrosis, and several additional candidates (including FGF21

* Corresponding authors. Addresses: QIMR Berghofer Medical Research Institute, Herston Rd, Herston, QLD 4006, Australia; (E. Powell), or Genomics and Machine Learning Laboratory, QIMRB National Centre for Spatial Tissue and AI Research, QIMR Berghofer Medical Research Institute, Herston Rd, Herston, QLD 4006, Australia; (Q.H. Nguyen), or Innate Immunity and Inflammation Group, Mater Research, Translational Research Institute, Kent St, Woolloongabba, QLD 4102, Australia; (K. Irvine).
E-mail addresses: Elizabeth.Powell@qimrb.edu.au (E.E. Powell), Quan.Nguyen@qimrb.edu.au (Q.H. Nguyen), katharine.irvine@uq.edu.au (K.M. Irvine).
https://doi.org/10.1016/j.jhepr.2025.101657

analogues and GLP-1 agonists) are in late-stage clinical trials.[5] These candidates primarily have metabolic mechanisms of action, although FGF21 analogues also appear to have a direct antifibrotic effect.[6] Clearly, there is an urgent need for effective, safe, and affordable drugs to treat the progressive form of this complex liver disease, prevent serious liver-related complications, and improve cardiometabolic comorbidities. In the past, many compounds failed to achieve primary endpoints in phase III clinical trials, likely reflecting the heterogeneity of cell types involved in the disease process as well as their variable phenotype and functional status.[7] These cell states are shaped by their location (for example hepatocyte metabolic zonation[8]) and the intercellular crosstalk within the metabolic, inflammatory and pro-fibrotic microenvironment that drives progressive MASLD.

To understand the processes driving progressive fibrosis and identify novel therapeutic targets, more granularity about the exact location and nature of cell-to-cell interactions within the liver is needed, alongside a deeper understanding of the interconnected networks involving metabolism, inflammation and fibrosis. Advances in sequencing technology, particularly single-cell RNA-sequencing and spatial transcriptomics, provide an unprecedented opportunity to link tissue morphology with molecular profiles. Single-cell RNA-sequencing has been leveraged to generate novel insights in healthy and diseased liver, but few studies have taken advantage of spatial transcriptomics.[9–11] A spatial analysis of fibrosis progression in human liver is crucial, as fibrosis stage is the most significant predictor of liver-related morbidity and mortality. Here we generated Visium spatial transcriptomic data from liver biopsies of patients spanning the spectrum of MASLD to identify the major cell types and their potential interconnected activities within each tissue region, and how region-specific cellular content and phenotype change with disease stage. Furthermore, we spatially characterised ligand-receptor pairs (LRPs) to discover region-specific cellular crosstalk associated with inflammation and fibrosis during MASLD progression.

Materials and methods

This study was approved by the QIMR Berghofer Human Research Ethics Committee (Project No. 3924) and Metro South Health Governance (Approval Number SSA/2023/QMS/104139). Spatial transcriptomic data from formalin-fixed paraffin-embedded liver biopsy samples from 32 patients with MASLD[12] were generated using the 10X Visium (Fig. 1A) platform and analysed as detailed in the supplementary methods.

Liver histology was assessed by an experienced liver pathologist (A.D.C.) who was blinded to the clinical and transcriptomic data. Fibrosis stage was recorded using a modified Non-Alcoholic Steatohepatitis Clinical Research Network (NASH CRN) staging score[2] based on the extent of steatosis, inflammation, hepatocellular ballooning and fibrosis. Fibrosis was staged from 0 to 4 as follows: stage 1, zone 3 perisinusoidal only or portal/periportal only; stage 2, zone 3 perisinusoidal and portal fibrosis; stage 3, bridging fibrosis; and stage 4, cirrhosis. Stage 3 - bridging fibrosis – was subdivided into stage 3a (few [1 or 2] fibrous septa) and stage 3b (many [>2] fibrous septa), which has been shown to give a more uniform spread of fibrosis stage.[13] Fibrosis was then categorised as early (stages 0 and 1), intermediate (stages 2 and 3a) or late (stages 3b and 4) (Fig. 1B and S1A).

Results

Spatial transcriptomic resolution of histopathological features in MASLD

Spatial transcriptomic profiling was performed on liver biopsies from 32 patients with MASLD across the spectrum of disease severity (Figs. 1A and S1). Two synchronous liver biopsy cores (two passes) from a single patient were included to assess the reproducibility of the experimental approach. Of the 33 total liver biopsies, 14 biopsies exhibited no (stage 0) or minimal (stage 1) fibrosis, 5 had intermediate (stage 2, 3a) fibrosis, and 14 displayed severe fibrosis (stage 3b, 4) (Table S1, Fig. S1E). Our analysis was guided by relevant anatomical tissue regions defined by histopathological annotation and focused on changes associated with fibrosis stages (Fig. 1A,B). The mean number of Visium capture areas ("spots") per biopsy was 401. The number of genes per spot ranged from 800 to 1,500 (median 1,378), a common quality range for a spatial assay of archival formalin-fixed tissues.[14] When outliers were calculated using three median absolute deviations, none of the spots were considered outliers (Fig. S1A–C). Spots located on selected histopathological features were manually annotated based on the H&E-stained images of the respective sections (Fig. 1B and S1F). An average of 60% of spots per biopsy were annotated. Unsupervised clustering produced eight transcriptomically distinct clusters that highlighted corresponding annotated histopathological features, supported by defined gene markers (Fig. S1C and D). Non-linear dimensionality reduction, projected onto the uniform manifold approximation and projection (UMAP), assembled all spots into two main clusters (Fig. 1C, left and right), which were enriched for spots from biopsies with late (F3b, F4) and early/intermediate (F0, F1, F2, F3a) fibrosis, respectively. Late fibrosis spots exhibited a notable bimodal distribution in the UMAP, which was driven by genes associated with inflammation and extracellular matrix and metabolic processes on the left and right, respectively (Fig. S2). Focussing on histopathological annotations, the late fibrosis (left) cluster contained annotated spots related to fibrous septa, portal and lobular inflammation and the portal tract interface, whereas the early/intermediate fibrosis (right) cluster contained normal and steatotic hepatocytes (Fig. 1D). There was no observable difference in the distribution of ballooned hepatocytes (a cardinal feature of MASH) between the late and the early/intermediate clusters (Fig. 1D,E). There was a reduction in the proportion of spots annotated as normal hepatocytes, normal portal tracts, and steatosis with advancing fibrosis stage, while no spots in early-stage biopsies were annotated as 'fibrous septa' (Fig. 1E and S1F).

Cellular deconvolution based on single-cell RNA-sequencing from healthy and cirrhotic human liver was used to classify each spot into 12 cell types, including seven immune cell types, endothelial, epithelial (hepatocytes and cholangiocytes), mesenchymal (including hepatic stellate cells and myofibroblasts) and mesothelial cells, according to the majority cell type present (Fig. 1F,G and S3A,B).[15]

Transcriptome-based cellular deconvolution results showed that the distribution of the major cell types was well aligned with annotated histopathological features (Fig. 1F and S3A). For

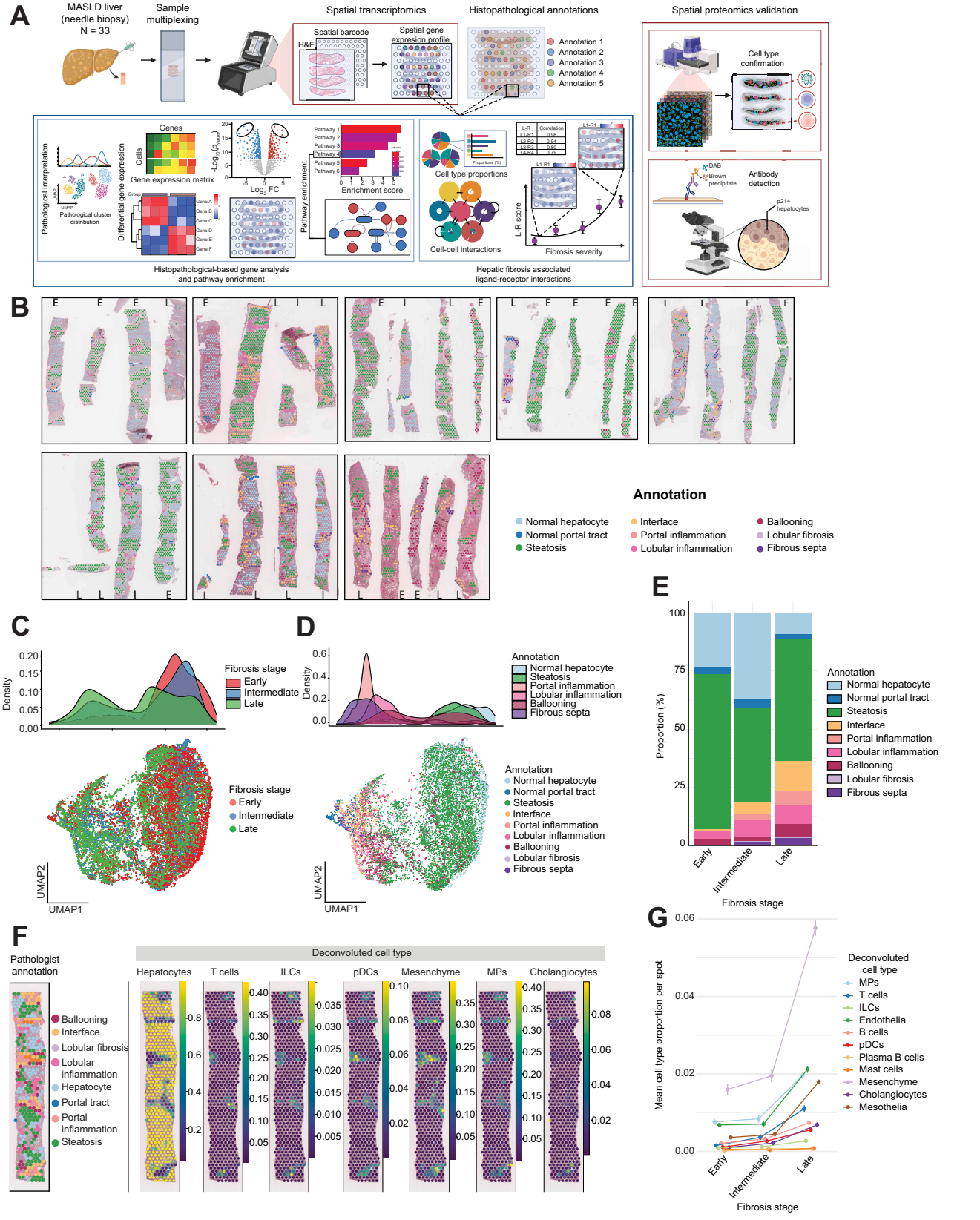

Fig. 1. Spatial resolution of gene expression in MASLD. 33 liver biopsies from 32 patients across the spectrum of MASLD severity were profiled by Visium spatial transcriptomics. (A) Project overview highlighting the experimental workflow and focus of analysis. (B) Biopsy-overlaid Visium spots coloured by histopathological annotation and labelled by fibrosis stage; E = early, I = intermediate and L = late. Annotated spots were clustered based on gene expression using unsupervised UMAP dimensionality reduction analysis and coloured according to (C) fibrosis stage and (D) histological annotation with histograms above UMAPs illustrating the

example, steatotic regions were identified as containing a majority of hepatocyte transcripts and portal areas contained cholangiocytes, mesenchyme and inflammatory cells (Fig. 1F). Although the majority of cells belonged to the hepatocyte annotation category across all patients (Fig. S3C), there was a significant increase in the proportion of spots attributed to T cells from early to late-stage fibrosis (Figs 1G and S3B-D).

Differential gene expression associated with specific histopathological features during MASLD progression

Significantly differentially expressed genes (DEGs) between early/intermediate- and late-stage fibrosis were identified via pseudo-bulk analysis for regions annotated as steatosis, inflammation (portal and lobular combined), portal tract interface, ballooning, normal hepatocytes and normal portal tracts (Fig. 2A and S4A,B). Sixteen genes enriched in early- and 36 genes in late-stage fibrosis were common to steatosis, inflammation, interface and ballooning comparisons (Fig. S4C and D). Portal and lobular inflammation had the highest number of DEGs compared to the other three categories. Comparisons between normal and steatotic hepatocytes demonstrated upregulation of lipid metabolism, fibrogenic, and immune-related genes in steatotic regions, reflecting transcriptional changes associated with early disease progression (Fig. S4E).

DEGs upregulated in late-stage fibrosis (in two or more anatomical groups, filtered to include only genes significant in at least two independent analyses, n = 277, Table S3) demonstrated a higher expression score in regions of portal and lobular inflammation, ballooned hepatocytes and portal interface than in normal and steatotic hepatocytes (Fig. 2B and S5A). This gene set was enriched for multiple reactome pathways related to extracellular matrix organisation (Fig. 2C and S6B). Gene set co-expression analysis (GeseCA) revealed strong co-expression between UMAP-clustered late fibrosis spots and several hallmark gene sets,[16] including epithelial-mesenchymal transition (EMT), TNF signalling via NF-kB, and other stress and inflammation pathways, which was clearly evident when the co-expression z-scores for each spot were projected onto the original UMAP (Fig. 2D and S4F). The reduced expression of the epithelial marker E-cadherin (*CDH1*) and gain of the mesenchymal marker vimentin (*VIM*) in the transition from early to late stage was spatially confirmed (Fig. 2E). CODEX proteomics analysis also demonstrated higher protein expression levels of VIM and lower levels of CDH1 (Fig. 2F). Collagen 4, CD163 and CD44, which were identified as upregulated in two or more annotation groups in late fibrosis (Table S3), were also upregulated at the protein level in late-stage fibrosis (Fig. 2F).

Upregulated DEGs for early/intermediate-stage fibrosis (in two or more anatomical groups, n = 304, Table S2) exhibited an inverse expression pattern compared to late-stage fibrosis DEGs in annotated regions across the liver biopsies (Fig. 2B, 3A, and S5B) and were significantly enriched for metabolic pathways, including amino acids, lipids, fatty acids, bile salts and xenobiotics (Fig. 3B and S6A). GeseCA also revealed strong co-expression of UMAP-clustered early-stage fibrosis spots and these physiological metabolic pathways (Fig. S4F). Glycolysis genes were strongly co-expressed with late-stage fibrosis, whereas genes involved in oxidative phosphorylation and fatty acid metabolism were enriched in early-stage fibrosis spots (Fig. 3C). The latter, along with the significant enrichment in the biological oxidations pathway among early-stage upregulated genes (Fig. 3B) and co-expression of genes related to reactive oxygen species in late fibrosis (Fig. 3C), may reflect impaired mitochondrial function and fatty acid oxidation associated with MASLD progression.[17] Analysis of a multi-platform serum metabolomics dataset for an extended cohort of 218 patients also revealed a reduction in fumaric acid, an intermediate metabolite in the tricarboxylic acid cycle, from early-to late-stage fibrosis (Fig. S7). The apparent changes in metabolic function may also reflect altered metabolic zonation, as has previously been suggested.[18,19] Broadly, oxygen-demanding processes such as gluconeogenesis, beta-oxidation and ammonia conversion to urea are higher in zone 1 (periportal), whereas glycolysis, lipid synthesis and ammonia conversion to glutamate are higher in zone 3 (pericentral) hepatocytes.[18] Consistent with a shift from portal-to central-dominant metabolic functions with disease progression, expression of the liver isoform of glutaminase (*GLS2*) and a rate-limiting enzyme of the urea cycle (*CPS1*) were increased in early-stage biopsies, whereas glutamine synthetase (*GLUL*) was upregulated in late-stage fibrosis (Tables S2–3). Gluconeogenic genes – including *FBP1*, which encodes the rate-limiting enzyme fructose-1,6-bisphosphatase 1, as well as *PCK1*, *ALDOB*, *G6PC*, and *ASS1*, which is involved in the metabolism of the urea cycle and the glucogenic amino acid arginine – were similarly enriched in early-stage fibrosis (Table S2). The switch from reliance on oxidative phosphorylation to glycolysis, known as the Warburg effect, is also frequently reported in other inflammatory states and cancer. Consistent with this, metabolic genes found to be upregulated in HCC[20] were enriched in late-stage fibrosis (Fig. 3D,E), whereas metabolic genes downregulated in HCC[20] were enriched in the early-stage fibrosis cluster, demonstrating lower expression in portal and lobular inflammatory regions (Fig. 3F,G). Taken together, these molecular signatures are consistent with the increase in matrix deposition and inflammatory signalling with MASLD progression, a concomitant decline in normal liver metabolic function, and significant reprogramming of metabolic fuel utilisation.

distribution of classified spots along the X axis. (E) Mean proportion of annotated spot types among early-, intermediate- and late-stage fibrosis biopsies. (F) Inferred deconvoluted cell type composition, displayed individually, demonstrated on a representative late-stage biopsy with scale bars representing the probability of each cell type being present in a specific location. The inferred cell types/composition align with the pathologist's annotation (far left in Fig. 1F). (G) Mean proportion of deconvoluted cell types predicted by CARD analysis. Proportion refers to the average representation of each cell type across multiple locations after the deconvolution process. All cell types showed a statistically significant (Benjamini/Hochberg adjusted *p* values for testing the linear regression slopes between cell proportions and fibrosis stages 9.06E-3 to 3.31E-220, lowest significance observed in mast cells) change in proportion from early-to late-stage fibrosis. Hepatocytes were excluded for visual clarity (see Fig. S3B). DC, dendritic cells; ILC, innate lymphoid cells; MASLD, metabolic dysfunction-associated steatotic liver disease; MP, mononuclear phagocytes; UMAP, uniform manifold approximation and projection.

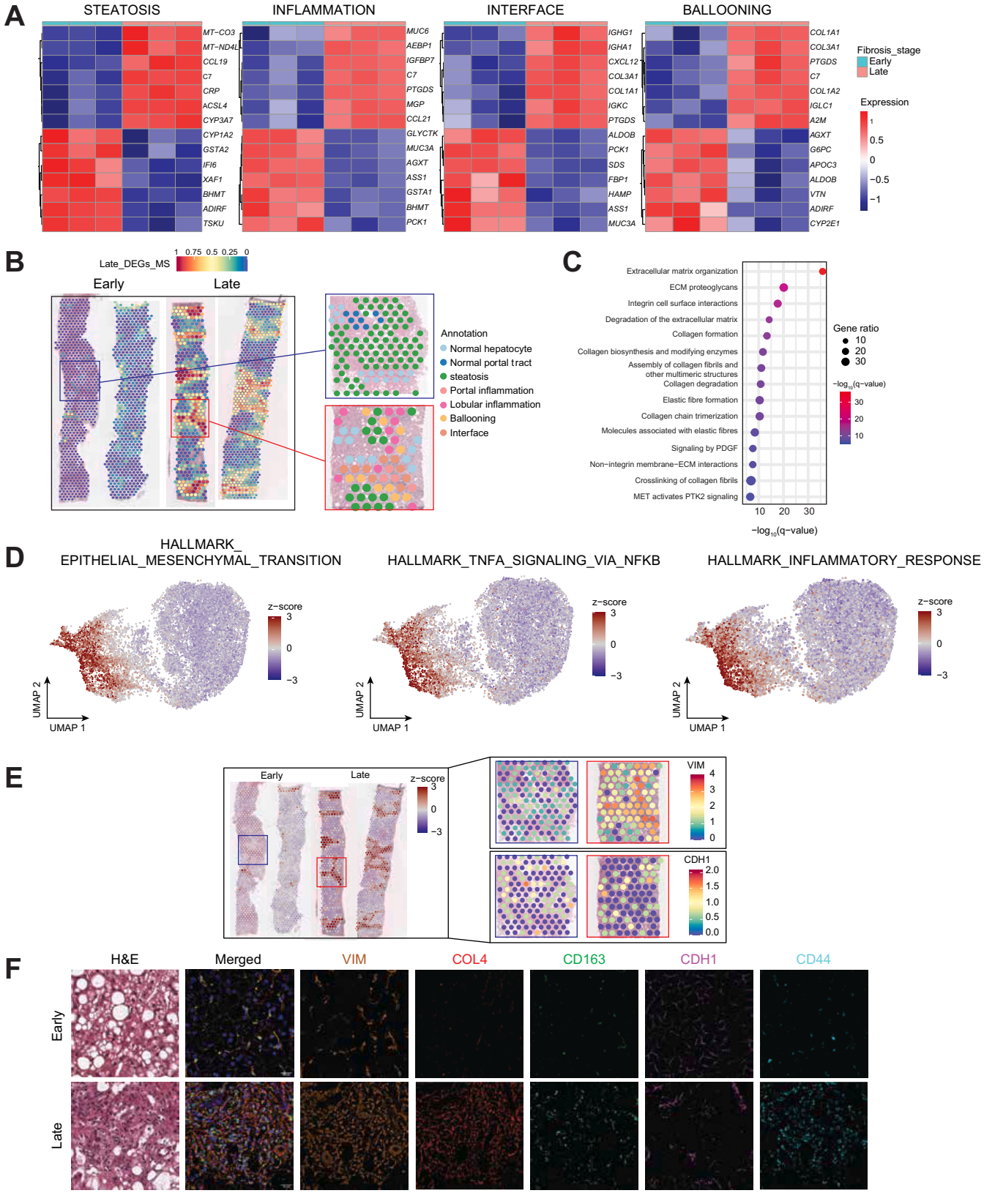

Fig. 2. Differential gene expression associated with specific histopathological features during MASLD progression. (A) Top seven DEGs between spots annotated as steatosis, portal or lobular inflammation, interface and ballooning in early- and late-stage fibrosis. (B) Representative examples of late-stage fibrosis-enriched DEGs present in two or more comparisons in early- and late-stage biopsies with spots coloured by gene expression. Scale bars represent module scores of all DEGs. Corresponding pathological annotations of selected regions of interest are shown. (C) Significantly enriched Reactome pathways for DEGs in late-stage

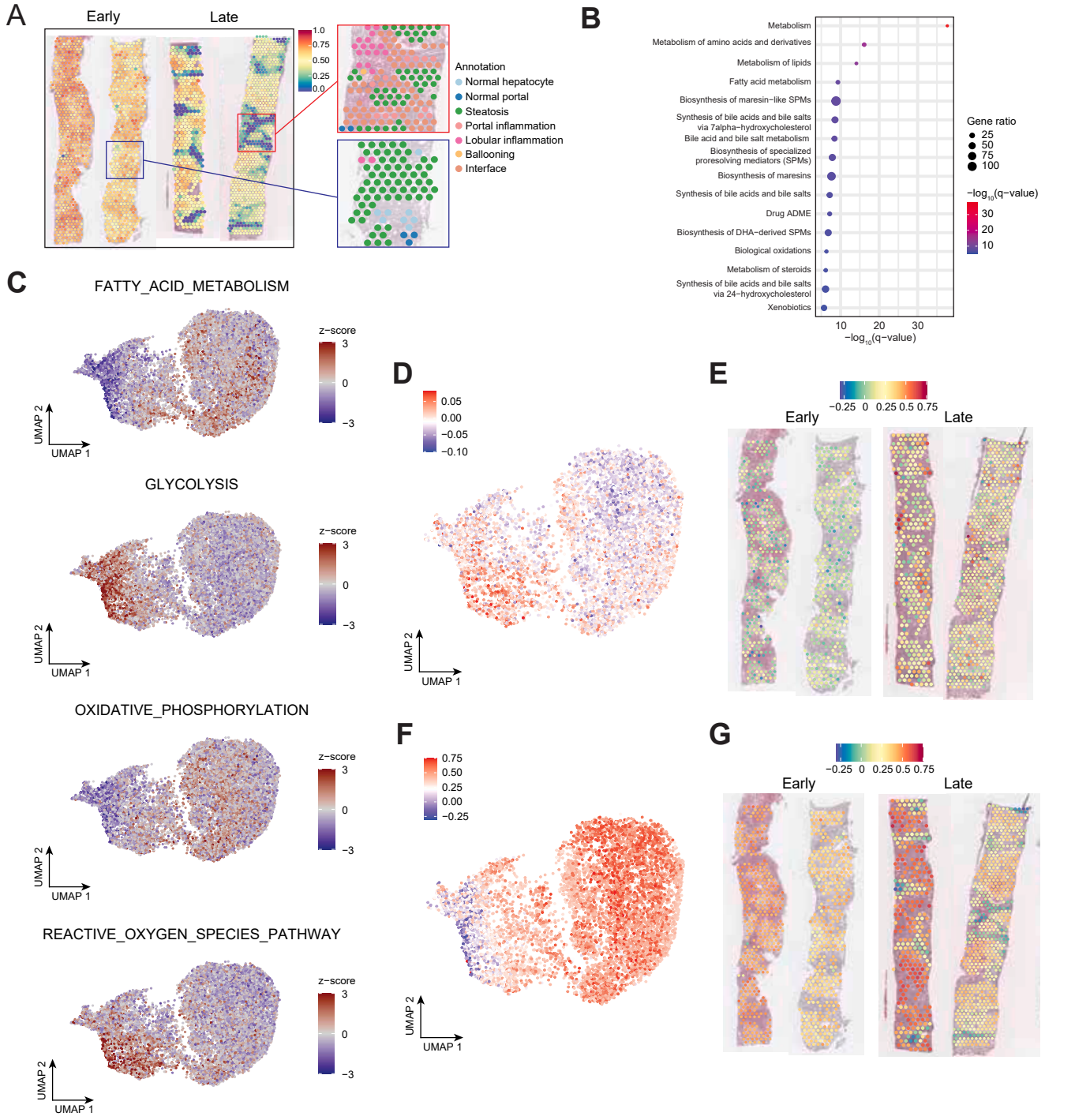

Fig. 3. MASLD progression is associated with metabolic reprogramming at a transcriptional level. (A) Representative examples of early-stage fibrosis-enriched DEGs present in two or more anatomical comparisons between early- and late-stage biopsies with spots coloured by gene expression. Scale bars represent module scores of all DEGs. Corresponding pathological annotations of selected regions of interest are shown. (B) Significantly enriched Reactome pathways for DEGs in early-stage fibrosis (geohypermetric test, p <0.01). (C) Gene set co-expression scores for the metabolic-related hallmark gene set projected onto the UMAP. Expression of metabolic genes identified as (D, E) up- or (F, G) downregulated in HCC for each spot visualised by (D,F) UMAP clustering and (E,G) biopsy location. DEGs, differentially expressed genes; HCC, hepatocellular carcinoma; MASLD, metabolic dysfunction-associated steatotic liver disease; UMAP, uniform manifold approximation and projection.

fibrosis (hypergeometric test, p <0.01). (D) Three hallmark gene sets selected from the 10 most enriched gene sets. Gene set co-expression scores were projected onto the UMAP and coloured by the scores. (E) Example spatial expression of the epithelial-mesenchymal transition gene set and the top two related markers: vimentin (*VIM*) and E-cadherin (*CDH1*) in early- and late-stage biopsies. (F) Examples of CODEX (co-detection by indexing) stains with VIM, collagen 4 (COL4), CD163, CDH1 and CD44 protein expression detected by CODEX analysis. Scale bar = 20 μm. DEGs, differentially expressed genes; MASLD, metabolic dysfunction-associated steatotic liver disease; UMAP, uniform manifold approximation and projection.

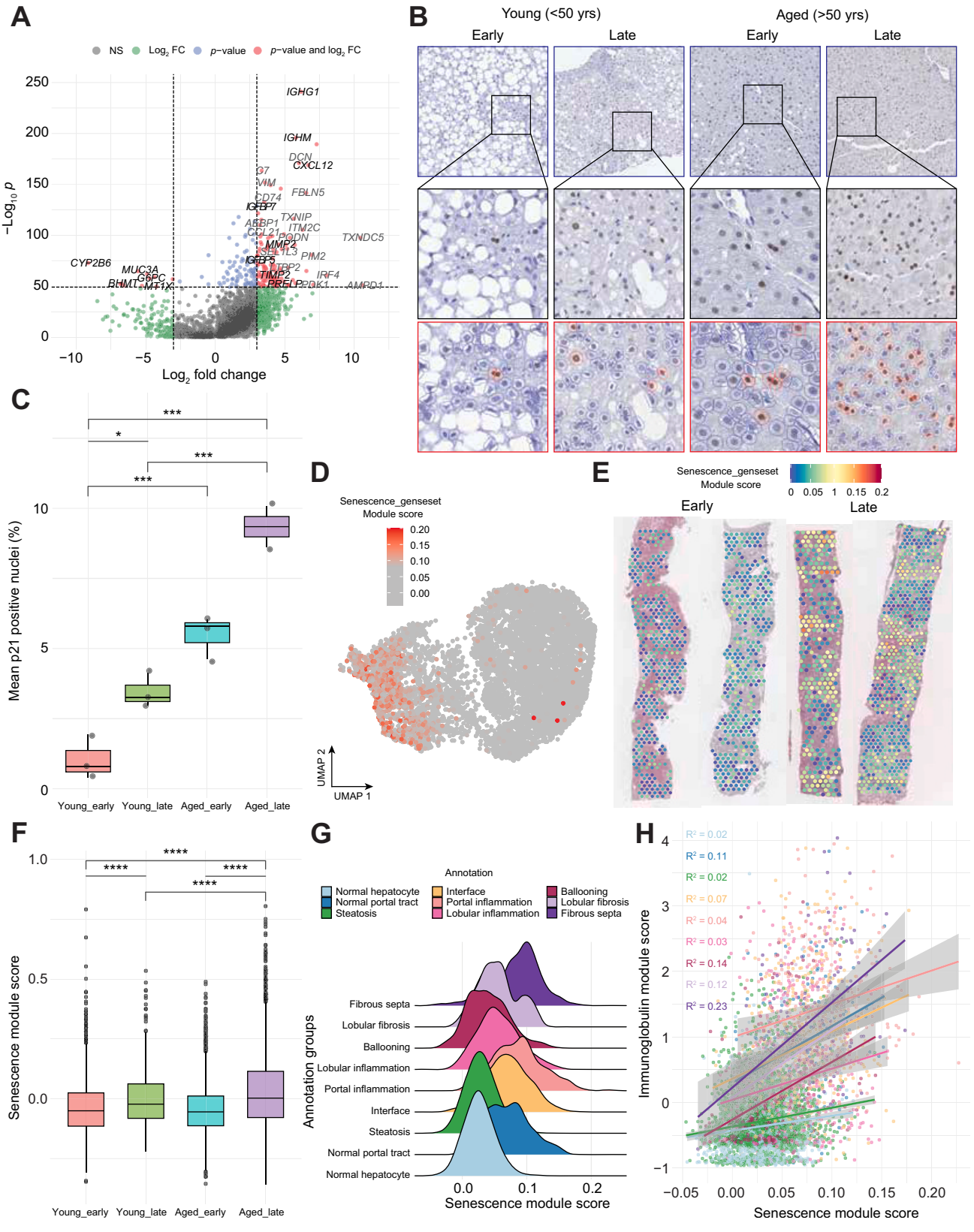

Fig. 4. MASLD progression is associated with increasing cellular senescence. (A) Differentially expressed genes between spots with the highest and lowest predicted immunoglobulin expression. (B) Immunohistochemistry staining for p21 on representative young (≤ 50 years) and aged (>50 years) samples for early- and late-stage fibrosis. Quantification was performed using QuPath's Positive Cell Detection tool, with detected cells outlined in blue and cells with p21+ nuclei outlined in red. (C) Bar plot showing the mean percentage of p21-positive nuclei per biopsy, grouped by age and fibrosis stage. Error bars represent standard deviation.

MASLD progression is associated with increased immunoglobulin expression and senescence

Several genes encoding immunoglobulins (*IGKC, IGHG, IGHA, IGLC*) were upregulated in late-stage fibrosis at the portal tract interface and in regions containing ballooned hepatocytes (Fig. 2A). Ma *et al.* (2024) recently reported immunoglobulin and complement expression co-localised with accumulating senescence 'hotspots' in aged tissues, including mouse and human liver.[21] Cellular senescence is also a feature of chronic liver disease, including MASLD.[22] We therefore hypothesised that immunoglobulin gene expression would be spatially associated with a senescence signature in MASLD biopsies. DEGs between spots with a high immunoglobulin module score (comprising *IGKC, IGHG, IGHA, IGLC*) and those with a low score included several genes previously implicated in the senescence-associated secretory phenotype (SASP) across various tissues, such as *TGFB1*, *TIMP2*, *MMP2*, *IGFBP7* and *CXCL12*[23,24](Fig. 4A). *CDKN1A*, encoding the canonical senescence-associated cell cycle inhibitor p21, was upregulated in late fibrosis (Table S3), and significantly increased at the protein level in hepatocyte nuclei in late-stage biopsies (Fig. 4B,C). As expected, p21 expression was also associated with increased age, regardless of fibrosis stage (Fig. 4B,C). We created an integrated senescence signature based on the SenMayo[23] and Gene Ontology Bioprocess gene sets (Table S5). The senescence signature was enriched in inflammatory and fibrotic regions when projected onto the original UMAP and represented spatially (Fig. 4D,E). Despite the age-dependent increase in p21 staining regardless of fibrosis stage (Fig 4C), the mean senescence module score was similarly low in early-stage biopsies, with a stepwise increase in patients <50 and >50 with late-stage fibrosis (Fig 4F), indicating an association with fibrosis across age groups. Consistent with an association between senescence and immunoglobulin expression, there was a positive correlation between the senescence gene module score and the immunoglobulin module score within each spot, with the highest correlation in the fibrous septa (Fig. 4H). Consistently, the mean senescence module score was highest in fibrous septa, along with portal inflammation (Fig. 4G). Despite the increase in immunoglobulin expression, our cell deconvolution analysis did not detect any enrichment of plasma cells, likely due to the relatively small proportion of these cells (Fig. 1G) and consistent with a previous report.[21] However, there was a positive correlation between the presence of plasma cell markers (Table S5, not including immunoglobulins themselves) and the immunoglobulin module score (Fig. S9A and B), suggesting an association between these features. Unsupervised clustering of Visium spots also revealed a close association between immunoglobulins and JCHAIN, which is largely expressed by plasma cells (Fig. S1C and D). Spatial mapping of plasma cells at the protein level (CODEX) also showed strong alignment with the Visium immunoglobulin module score (Fig. S9C–F). Senescence in MASLD has previously been linked with similar hepatic metabolic perturbations to those identified by our differential gene expression and GeseCA analyses (Fig. 3), as well as to the development of HCC, with the gluconeogenic gene *FBP1* increasingly implicated as an important tumor suppressor. Together, the data demonstrate coincident increases in transcriptomic signatures of inflammation, fibrosis and senescence, immunoglobulin gene expression and nuclear p21 expression in hepatocytes with MASLD progression.

Co-regulated ligand-receptor pairs associated with MASLD fibrosis progression

To gain further insight into the cellular and molecular interactions driving fibrosis progression in MASLD, we applied an unbiased, high-throughput screening approach to identify LRPs that were statistically enriched for spatial co-expression within Visium spots, using a spatially-constrained two-level permutation test implemented in stLearn.[25] To ensure comprehensiveness, we utilised connectome DB2020, which consists of 2,293 manually curated LRPs with literature support.[26] Ligand-receptor scores between neighbouring cells, reflecting the probability and strength of interactions, were tested for significant correlation with fibrosis stages, suggesting increasing or decreasing interactions with progression from early to late fibrosis (Fig. 5A,B). Fibrosis-associated LRPs included extracellular matrix components (collagens interacting with *CD44*, *CD36* and *DDR2*, and the proteoglycans decorin [*DCN*] and biglycan [*BGN*] interacting with *TLR2*) and modulators (*e.g. TIMP1-CD63*) and inflammatory chemokines, cytokines and receptors (*e.g. SPP1-ITGAV*, *CXCL12-CD4*, *CLEC11A-ITGB1*) (Fig. 5C,D). Of those, the predicted interaction between *TIMP1-CD63* was most strongly correlated with fibrosis progression (Fig. 5C,D and S8A), consistent with the previous report that this interaction drives fibrosis by activating the PI3K/Akt survival pathways and preventing apoptosis of activated fibroblasts and hepatic stellate cells.[27,28] Examples of LRPs with higher activity in early disease included *RTN4* and its receptor, *ANGPTL3-ITGAV*, and ephrin A1 (*EFNA1*) and its receptors *EPHA1* and *EPHA2* (Fig. 5C,E and S8B). The LRP analysis was then confined to portal inflammation annotated spots, to identify candidate LRPs driving inflammation in this key region. The LRPs most highly correlated with fibrosis stage included inflammatory mediators such as *CXCL12-ACKR3*, *SEM4AD-PLXNB2* and *LTB-LTBR* (Fig. 5F). Several LRPs in portal inflammation spots were inversely correlated with fibrosis, including signalling pathways such as *C3-CR1*, *MIF-CD74*, and *LGALS9-CD44* (Fig. 5G). The chemokine *CXCL12* was a component of nine of the 145 LR pairs associated with increasing fibrosis stage, including seven of the top 50. Although *CD4* was the most highly correlated candidate receptor, *CXCL12*'s canonical signalling receptors *CXCR4* and

Statistical comparisons were performed using one-way ANOVA followed by Tukey's HSD *post hoc* test. Statistical significance was denoted as follows: $p \leq 0.05$ (*), $p \leq 0.01$ (**), $p \leq 0.001$ (***). Senescence gene expression score (D) projected onto the UMAP plot and (E) plotted spatially on representative early- and late-stage biopsies. (F) Bar plot showing senescence gene expression score, grouped by age and fibrosis stage. Error bars represent standard deviation. Statistical comparisons were performed using one-way ANOVA followed by Tukey's HSD *post hoc* test. Statistical significance was denoted as follows: $p \leq 0.0001$ (****). (G) Ridge plot showing mean module score for expression of senescence genes, grouped by annotation. Colours for each annotation correspond to those shown in panel. (H) Spearman correlation between the average expression of the genes in the senescence module and immunoglobulin module score for each spot. FC, fold-change; MASLD, metabolic dysfunction-associated steatotic liver disease; UMAP, uniform manifold approximation and projection.

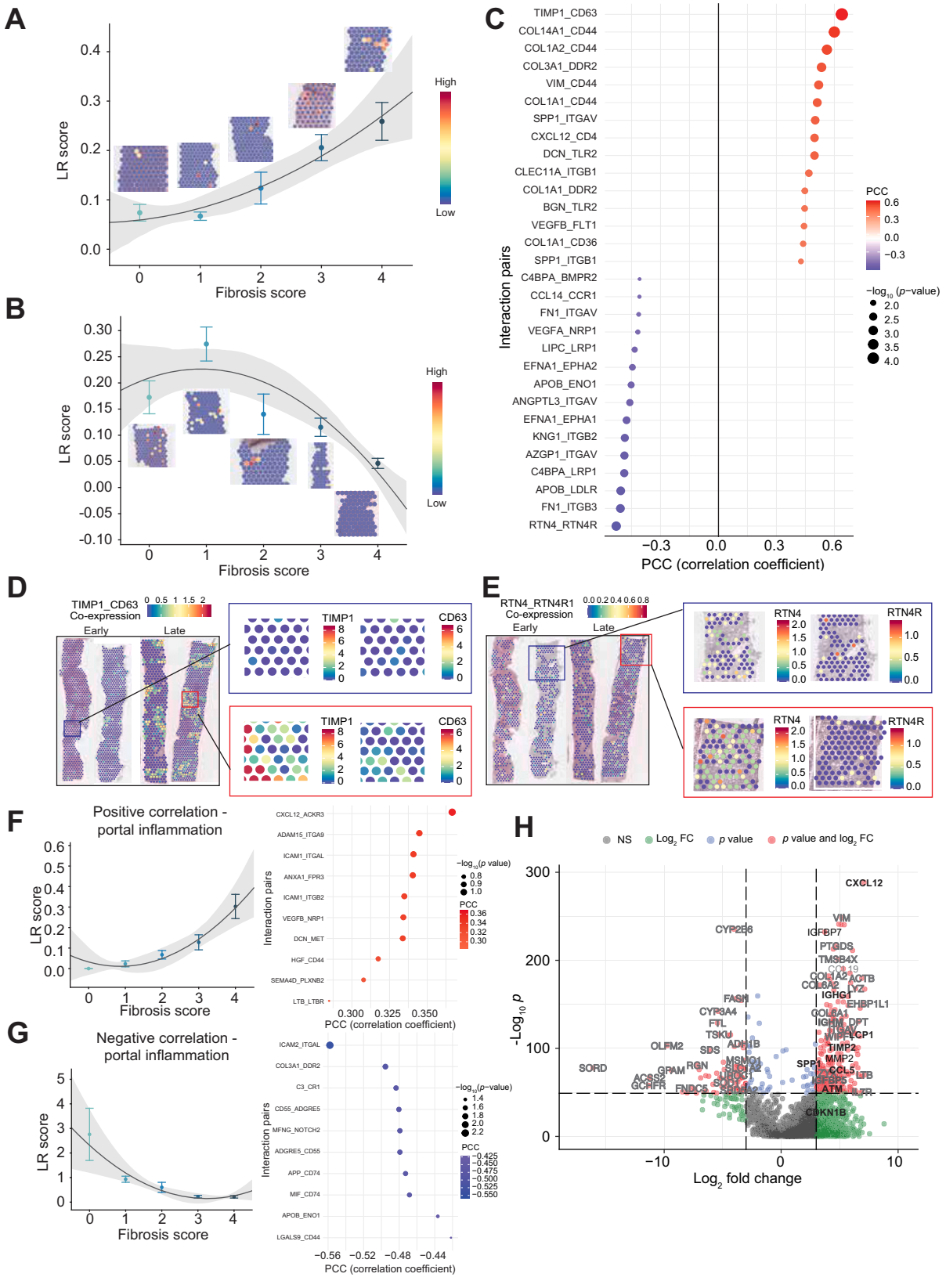

Fig. 5. Co-regulated ligand-receptor pairs associated with MASLD fibrosis progression. LR pair interactions were predicted based on co-expression by neighbouring cells within spots and assigned an LR score based on the strength of the prediction. LR pairs that (A) positively or (B) negatively correlated with fibrosis stage were identified with error bars showing standard error. (C) Top 15 LR pairs correlated with fibrosis progression shown by gradient scale from blue to red, with -log(*p* value) represented by the size of dots. The *p* values were derived from testing for linear regression slopes between LR scores and fibrosis stages, corrected by

CXCR7 (*ACKR3*) were also identified, along with several integrins (Fig. 5C). *CXCL12* is one of a number of chemokines that have been reported as part of the SASP, though not specifically in the liver. We identified DEGs between spots with the highest and lowest scores for *CXCL12* interaction with any putative receptor (top and bottom 10%, respectively). Genes associated with high *CXCL12*-receptor activity included other SASP genes, such as *IGFBP7*[29] and *CCL5*, along with immunoglobulins and the known pro-fibrotic cytokine osteopontin (SPP1) (Fig. 5H).

Discussion

The development of progressive fibrosis in MASLD involves dynamic cellular interactions within the highly structured microenvironment of hepatic lobules. The liver's complex organisation and pleiotropic metabolic functions have led to difficulty in achieving effective drug therapies for MASLD fibrosis. In this study we demonstrated that MASLD progression is associated with upregulation of a senescence gene expression signature and p21 expression in hepatocytes, increased immunoglobulin gene expression, and concomitant perturbation of hepatic metabolic pathways.

Not surprisingly, as fibrosis progressed there was an overall increase in mesenchyme, mononuclear phagocytes, T cells and cholangiocytes, with an upregulation in genes enriched for extracellular matrix/receptor interactions (*MGP*, *COL3A1*, *COL1A1*, *COL1A2*), and immune cell recruitment and trafficking (*CCL19*, *CCL21*, *CXCL12*). In particular, these transcripts were among the most highly differentially expressed genes in the portal tract interface and regions containing ballooned hepatocytes that release inflammatory and fibrogenic signals. Gene sets highly correlated with genes regulated during MASLD progression include TNF signalling, reflecting the strong inflammatory basis of the process, and EMT, previously proposed as a possible driver of liver fibrosis. We[30] and others[31] identified that the ductular reaction, a complex of strings of cholangiocytes and bile ductules, in a niche of stromal and inflammatory cells at the portal tract interface, correlates with the extent of fibrosis in MASLD. As well as producing factors that lead to increased extracellular matrix, ductular cells share some properties of mesenchymal cells,[32] although whether they are generated via EMT remains unclear.[33]

As fibrosis progressed, the differential expression of ligand-receptor signalling pairs revealed cell-cell communication networks dominated by extracellular matrix components/modulators and inflammatory chemokines, cytokines and receptors. Interacting cells likely include a combination of the increasing contribution of infiltrating cells to hepatocyte-dominated spot composition as inflammation and fibrosis progress and induction of new expression in hepatocytes in response to the microenvironment. LRPs that correlated with fibrosis progression included recognised drivers of fibrosis such as osteopontin,[34] vimentin[35] and *CXCL12*,[36] illustrating the redundancy in inflammatory and fibrogenic signalling.[37] The chemokine *CXCL12* featured in nine interactions within LRPs that correlated with fibrosis severity (*CD4*, *ITGA4*, *ITGAV*, *ITGB1*, *CXCR4*, *ITGA5*, *ACKR3*, *ITGA5*, *ITGB3*), with different interactions dominating in specific histopathological regions. The CXCL12 signalling axis regulates the migration and activation of leucocytes, endothelial cells, and stem cells through binding to CXCR4, which activates G-protein signalling, and to the scavenging receptor ACKR3, which signals via the β-arrestin-2 pathway. Mouse models of chronic liver injury suggest that the *ACKR3* and *CXCR4* pathways have differential effects on liver repair and fibrosis, respectively. Inhibiting the *CXCL12-CXCR4* pathway did not reduce fibrosis,[36] whereas blockade of *CXCR4*-mediated inflammation counteracted age-related senescence and steatosis and mitigated diet-induced MASLD.[38] More recently, *CXCL12* has been reported to activate integrins in a rapid, receptor-independent manner,[39] suggesting a role in modulating leucocyte extravasation. Our data also support the relevance of this chemokine in human MASLD, and the need for more detailed investigations into the roles of *CXCL12-CXCR4* signalling in liver fibrosis.

Our study provides further insight into the possible factors that may be driving this marked inflammatory and fibrogenic response. Unexpectedly, genes encoding immunoglobulins (*IGKC, IGHG1, IGHA1, IGLC1*) were among the top eight genes differentially expressed between early- and late-stage fibrosis at the portal tract interface and in regions containing ballooned hepatocytes. Although not previously reported in MASLD, immunoglobulin-related genes were the most highly upregulated DEGs in senescent regions of aged tissues in mice, and were reported to reinforce senescence.[21] The functional implications of immunoglobulin expression in the liver are unknown, but accumulation of IgG proteins in adipose tissue in aging mice caused inflammation and insulin resistance by competing for insulin receptor binding.[40,41] We also identified a positive correlation between immunoglobulin gene expression and senescence in our human MASLD liver biopsies; multiple components of the SASP including *TGFB1*, *TIMP2*, *MMP2*, *IGFBP7* and *CXCL12* were enriched in late-stage fibrosis along with nuclear p21. Although there is significant overlap among senescence, inflammation and fibrosis gene expression signatures, the data are consistent with an accumulation of senescent cells, which has previously been reported in MASLD,[22] and may be a common feature among fibrotic diseases.[42] Whether senescence is a cause or a consequence of disease progression is not clear. In mice, inducing hepatocyte senescence was sufficient to promote liver fat accumulation, and elimination of senescent cells reduced age-associated hepatic steatosis.[43] However, the most widely studied senolytic drugs dasatinib and quercetin had limited impact on hepatic senescence and did not reduce MASLD progression.[44,45] Moreover, it is possible that targeting senotherapeutic strategies towards distinct senescent cell types will be important to remove or

Benjamini/Hochberg false discovery rate method. (D,E) Spatial visualisation of the top LR pairs positively (*TIMP1-CD63*) and negatively (*RTN4-RTN4R1*) correlated with fibrosis stage. LR pair interactions were predicted based on co-expression within spots annotated as portal inflammation and assigned an LR score based on the strength of the prediction. LR pairs (F) positively or (G) negatively correlated with fibrosis stage were identified. (H) Differentially expressed genes between spots with the highest and lowest predicted *CXCL12*-receptor activity for all identified interacting receptors. LR, ligand-receptor; MASLD, metabolic dysfunction-associated steatotic liver disease.

counteract their effect in specific contexts, in order to reduce liver injury and improve immunosurveillance.[46]

Our data show marked dysregulation in metabolic pathways with increasing fibrosis, particularly in regions defined by inflammation, ballooning and at the portal tract interface. Late-stage fibrosis was associated with increased expression of glycolysis, which is a key feature of senescent cells,[47] but also activated hepatic stellate cells and inflammatory macrophages.[46,48] Several of the genes expressed at low levels in late-stage fibrosis (*ALDOB*, *FBP1*, *PCK1*, *BHMT*, *GSTA1*, *ASS1*, *AGXT*, *GLYCTK*, *G6PC*) likely reflect metabolic adaptations in cellular substrate metabolism during disease progression, which in turn influence the activation of inflammatory and fibrogenic cells.[11,20,46–49] For example, the zone 1 (portal) gluconeogenic enzyme FBP1 antagonises glycolysis, but hepatocyte-specific deletion of *Fbp1* also promoted stellate cell activation, senescence, fibrosis and carcinogenesis in rodent models, potentially mediated via the alarmin HMGB1.[46] Another recent report identified *FBP1* as a p53 target, which was suppresed in pre-malignant senescent hepatocytes, but re-activated in malignant hepatocytes to enhance activity of previously senescent cells, thereby facilitating carcinogenesis.[50] Age is a major risk factor for MASLD, so disease-linked metabolic remodeling may in part be related to parallel age-related tissue changes including senescence and shifts in liver zonation that have been reported in both mice and humans.[21,43] Here we identified reduced expression of periportal genes, such as *CDH1, GLS2*, *CPS1*, and gluconeogenic genes including *FBP1*, with concomitant upregulation of the pericentral *GLUL*, during progression from early-to late-stage fibrosis. Targeting these metabolic adaptations that drive inflammatory and fibrogenic cellular responses may have therapeutic benefit in MASLD;[48] however, cell type- and context-specific targeting of metabolic pathways will likely be crucial to minimise off-target events.

Our unbiased spatial analysis provides an integrated view of molecular pathway alterations and cellular interactions spanning the spectrum of MASLD. We identify metabolic perturbations and increasing senescence and inflammatory pathways that are significantly linked to fibrosis progression. These candidate molecules warrant validation through independent cohorts and functional perturbation models.

Affiliations

[1]*QIMR Berghofer Medical Research Institute, Brisbane, QLD, Australia;* [2]*Institute for Molecular Bioscience, The University of Queensland, Brisbane, QLD, Australia;* [3]*Department of Pharmacology, University of Oxford, Oxford, United Kingdom;* [4]*Turku Bioscience Centre, University of Turku and Åbo Akademi University, Turku, Finland;* [5]*Department of Chemistry, University of Turku, Turku, Finland;* [6]*School of Science and Technology, Örebro University, Örebro, Sweden;* [7]*Department of Life Technologies, University of Turku, Turku, Finland;* [8]*School of Medical Sciences, Faculty of Medicine and Health, Örebro University, Örebro, Sweden;* [9]*Kidney Health Service, Metro North, Brisbane, QLD, Australia;* [10]*Department of Anatomy and Physiology, The University of Melbourne, Melbourne, Victoria, Australia;* [11]*Centre for Liver Disease Research, Faculty of Medicine, Translational Research Institute, The University of Queensland, Brisbane, QLD, Australia;* [12]*Mater Research, The University of Queensland, Translational Research Institute, Brisbane, QLD, Australia;* [13]*Department of Gastroenterology and Hepatology, Princess Alexandra Hospital, Brisbane, QLD, Australia*

Abbreviations

DEGs, differentially expressed genes; EMT, epithelial-mesenchymal transition; GeseCA, gene set co-expression analysis; HCC, hepatocellular carcinoma; LRPs, ligand-receptor pairs; MASLD, metabolic dysfunction-associated steatotic liver disease; SASP, senescence-associated secretory phenotype; UMAP, uniform manifold approximation and projection.

Financial support

EEP was supported by a QLD Health Targeted Clinical Research Fellowship. KMI is grateful for core laboratory funding from the Mater Foundation. QHN is supported by the NHMRC Investigator Grant (GNT2008928), the QIMRB National Centre for Spatial Tissue and AI Research (NCSTAR), and the ACRF Centre for Optimised Cancer Therapy (COCT).

Conflict of interest

The authors do not have any conflicts of interest to report.
Please refer to the accompanying ICMJE disclosure forms for further details.

Authors' contributions

Hani Vu: Investigation, Data Curation, Formal Analysis, Visualization, Conceptualisation, Writing - Original Draft; Yuliangzi Sun: Formal Analysis, Visualization; Zherui Xiong: Investigation, Writing - Original Draft; Xiao Tan: Formal Analysis, Visualization, Writing – Review and Editing; Daniel Radford-Smith: Formal Analysis, Investigation, Writing - Original Draft; Andrew Causer: Formal Analysis; Alex M. Dickens, Tuulia Hyötyläinen, Matej Oresic & Ilia Evstafev: Investigation and Formal Analysis; Christian Nefzger, Eoin D. O'Sullivan, Matthew J. Watt & Grant Ramm: Writing - Review & Editing; Andrew Clouston: Conceptualisation, Investigation, Writing - Review & Editing; Katharine Irvine, Quan H. Nguyen & Elizabeth E. Powell: Supervision, Funding Acquisition, Resources, Conceptualisation, Project Adminisatration and Writing - Original Draft.

Data availability

Raw spatial transcriptomics data and tissue images have been uploaded to the open-access UQeSpace repository, available at https://doi.org/10.48610/e95155f. Single-cell RNA-sequencing (scRNA-seq) of healthy and cirrhotic human liver, with raw sequencing data available at Gene Expression Omnibus (GEO) under accession GSE136103. The algorithms used for the analyses in this study are all publicly available. All code is available at https://github.com/BiomedicalMachineLearning/Liver.

Supplementary data

Supplementary data to this article can be found online at https://doi.org/10.1016/j.jhepr.2025.101657.

References

Author names in bold designate shared co-first authorship

[1] Powell EE, Wong VW, Rinella M. Non-alcoholic fatty liver disease. Lancet 2021;397:2212–2224.
[2] Kleiner DE, Brunt EM, Van Natta M, et al. Design and validation of a histological scoring system for nonalcoholic fatty liver disease. Hepatology 2005;41:1313–1321.
[3] Steinberg GR, Valvano CM, De Nardo W, et al. Integrative metabolism in MASLD and MASH: pathophysiology and emerging mechanisms. J Hepatol 2025;83:584–595.
[4] Huang DQ, Wong VWS, Rinella ME, et al. Metabolic dysfunction-associated steatotic liver disease in adults. Nat Rev Dis Primers 2025;11:14.
[5] Healey N. The trials that could transform treatment for serious liver disease. Nat Med 2025;31:1720–1721.
[6] Harrison SA, Rolph T, Knott M, et al. FGF21 agonists: an emerging therapeutic for metabolic dysfunction-associated steatohepatitis and beyond. J Hepatol 2024;81:562–576.

[7] Tacke F, Puengel T, Loomba R, et al. An integrated view of anti-inflammatory and antifibrotic targets for the treatment of NASH. J Hepatol 2023;79:552–566.
[8] Kietzmann T. Metabolic zonation of the liver: the oxygen gradient revisited. Redox Biol 2017;11:622–630.
[9] **Perry AS**, **Hadad N**, **Chatterjee E**, et al. A prognostic molecular signature of hepatic steatosis is spatially heterogeneous and dynamic in human liver. Cell Rep Med 2024;5:101871.
[10] **Watson BR**, **Paul B**, Rahman RU, et al. Spatial transcriptomics of healthy and fibrotic human liver at single-cell resolution. Nat Commun 2025;16:319.
[11] Li JZ, Yang L, Xiao MX, et al. Spatial and single-cell transcriptomics reveals the regional division of the spatial structure of MASH fibrosis. Liver Int 2025;45:e16125.
[12] Patel P, Hossain F, Horsfall LU, et al. A pragmatic approach identifies a high rate of nonalcoholic fatty liver disease with advanced fibrosis in diabetes clinics and at-risk populations in primary care. Hepatol Commun 2018;2:893–905.
[13] Pai RK, Jairath V, Hogan M, et al. Reliability of histologic assessment for NAFLD and development of an expanded NAFLD activity score. Hepatology 2022;76:1150–1163.
[14] Vo T, Prakrithi P, Jones K, et al. Assessing spatial sequencing and imaging approaches to capture the molecular and pathological heterogeneity of archived cancer tissues. J Pathol 2025;265:274–288.
[15] Ramachandran P, Dobie R, Wilson-Kanamori JR, et al. Resolving the fibrotic niche of human liver cirrhosis at single-cell level. Nature 2019;575:512–518.
[16] Liberzon A, Birger C, Thorvaldsdottir H, et al. The Molecular Signatures Database (MSigDB) hallmark gene set collection. Cell Syst 2015;1:417–425.
[17] Moore MP, Cunningham RP, Meers GM, et al. Compromised hepatic mitochondrial fatty acid oxidation and reduced markers of mitochondrial turnover in human NAFLD. Hepatology 2022;76:1452–1465.
[18] Martini T, Naef F, Tchorz JS. Spatiotemporal metabolic liver zonation and consequences on pathophysiology. Annu Rev Pathol 2023;18:439–466.
[19] Yakubovsky O, Afriat A, Egozi A, et al. A spatial transcriptomics atlas of live donors reveals unique zonation patterns in the healthy human liver. bioRxiv 2025;2025. 2002.2022.639181.
[20] Nwosu ZC, Megger DA, Hammad S, et al. Identification of the consistently altered metabolic targets in human hepatocellular carcinoma. Cell Mol Gastroenterol Hepatol 2017;4:303–323 e301.
[21] **Ma S**, **Ji Z**, **Zhang B**, et al. Spatial transcriptomic landscape unveils immunoglobin-associated senescence as a hallmark of aging. Cell 2024;187:7025–7044 e7034.
[22] Jun JH, Du K, Dutta RK, et al. The senescence-associated secretome of Hedgehog-deficient hepatocytes drives MASLD progression. J Clin Invest 2024;134.
[23] Saul D, Kosinsky RL, Atkinson EJ, et al. A new gene set identifies senescent cells and predicts senescence-associated pathways across tissues. Nat Commun 2022;13:4827.
[24] Lopes-Paciencia S, Saint-Germain E, Rowell M-C, et al. The senescence-associated secretory phenotype and its regulation. Cytokine 2019;117:15–22.
[25] Pham D, Tan X, Balderson B, et al. Robust mapping of spatiotemporal trajectories and cell-cell interactions in healthy and diseased tissues. Nat Commun 2023;14:7739.
[26] Hou R, Denisenko E, Ong HT, et al. Predicting cell-to-cell communication networks using NATMI. Nat Commun 2020;11:5011.
[27] Jung KK, Liu XW, Chirco R, et al. Identification of CD63 as a tissue inhibitor of metalloproteinase-1 interacting cell surface protein. EMBO J 2006;25:3934–3942.
[28] Murphy FR, Issa R, Zhou X, et al. Inhibition of apoptosis of activated hepatic stellate cells by tissue inhibitor of metalloproteinase-1 is mediated via effects on matrix metalloproteinase inhibition: implications for reversibility of liver fibrosis. J Biol Chem 2002;277:11069–11076.
[29] **Siraj Y**, **Aprile D**, Alessio N, et al. IGFBP7 is a key component of the senescence-associated secretory phenotype (SASP) that induces senescence in healthy cells by modulating the insulin, IGF, and activin A pathways. Cell Commun Signal 2024;22:540.
[30] Gadd VL, Skoien R, Powell EE, et al. The portal inflammatory infiltrate and ductular reaction in human nonalcoholic fatty liver disease. Hepatology 2014;59:1393–1405.
[31] Guillot A, Winkler M, Silva Afonso M, et al. Mapping the hepatic immune landscape identifies monocytic macrophages as key drivers of steatohepatitis and cholangiopathy progression. Hepatology 2023;78:150–166.
[32] Gupta V, Sehrawat TS, Pinzani M, et al. Portal fibrosis and the ductular reaction: pathophysiological role in the progression of liver disease and translational opportunities. Gastroenterology 2024;168:675–690.
[33] Xie G, Diehl AM. Evidence for and against epithelial-to-mesenchymal transition in the liver. Am J Physiol Gastrointest Liver Physiol 2013;305:G881–G890.
[34] **Han H**, **Ge X**, Komakula SSB, et al. Macrophage-derived osteopontin (SPP1) protects from nonalcoholic steatohepatitis. Gastroenterology 2023;165:201–217.
[35] Wang PW, Wu TH, Lin TY, et al. Characterization of the roles of vimentin in regulating the proliferation and migration of HSCs during hepatic fibrogenesis. Cells 2019;8.
[36] Liepelt A, Tacke F. Stromal cell-derived factor-1 (SDF-1) as a target in liver diseases. Am J Physiol Gastrointest Liver Physiol 2016;311:G203–G209.
[37] Wang S, Li K, Pickholz E, et al. An autocrine signaling circuit in hepatic stellate cells underlies advanced fibrosis in nonalcoholic steatohepatitis. Sci Transl Med 2023;15. eadd3949.
[38] **Duan JL**, **Liu JJ**, **Ruan B**, et al. Age-related liver endothelial zonation triggers steatohepatitis by inactivating pericentral endothelium-derived C-kit. Nat Aging 2023;3:258–274.
[39] Fujita M, Davari P, Takada YK, et al. Stromal cell-derived factor-1 (CXCL12) activates integrins by direct binding to an allosteric ligand-binding site (site 2) of integrins without CXCR4. Biochem J 2018;475:723–732.
[40] Yu L, Wan Q, Liu Q, et al. IgG is an aging factor that drives adipose tissue fibrosis and metabolic decline. Cell Metab 2024;36:793–807 e795.
[41] Yu L, Yang YX, Gong Z, et al. FcRn-dependent IgG accumulation in adipose tissue unmasks obesity pathophysiology. Cell Metab 2024;37:656–672.
[42] **Velu PP**, **Abhari RE**, Henderson NC. Spatial genomics: mapping the landscape of fibrosis. Sci Transl Med 2025;17. eadm6783.
[43] Ogrodnik M, Miwa S, Tchkonia T, et al. Cellular senescence drives age-dependent hepatic steatosis. Nat Commun 2017;8:15691.
[44] Hense JD, Garcia DN, Zanini BM, et al. MASLD does not affect fertility and senolytics fail to prevent MASLD progression in male mice. Sci Rep 2024;14:17332.
[45] Islam MT, Tuday E, Allen S, et al. Senolytic drugs, dasatinib and quercetin, attenuate adipose tissue inflammation, and ameliorate metabolic function in old age. Aging Cell 2023;22:e13767.
[46] Li F, Huangyang P, Burrows M, et al. FBP1 loss disrupts liver metabolism and promotes tumorigenesis through a hepatic stellate cell senescence secretome. Nat Cell Biol 2020;22:728–739.
[47] Wiley CD, Campisi J. From ancient pathways to aging cells-connecting metabolism and cellular senescence. Cell Metab 2016;23:1013–1021.
[48] Horn P, Tacke F. Metabolic reprogramming in liver fibrosis. Cell Metab 2024;36:1439–1455.
[49] **Xu JX**, **Qin SL**, **Wei HW**, et al. Down-regulation of ALDOB during metabolic reprogramming mediates malignant behavior in hepatocellular carcinoma and insensitivity to postoperative adjuvant transarterial chemoembolization. Clin Sci (Lond) 2023;137:303–316.
[50] **Gu L**, **Zhu Y**, Nandi SP, et al. FBP1 controls liver cancer evolution from senescent MASH hepatocytes. Nature 2025;637:461–469.

Keywords: Liver; Senesence; Spatial Transcriptomics; Steatosis; Fibrosis; Metabolism; MASLD; inflammation.
Received 16 July 2025; received in revised form 17 October 2025; accepted 22 October 2025; Available online 4 November 2025